Marquette University
e-Publications@Marquette

Chemistry Faculty Research and Publications | Chemistry, Department of

4-2006

Styrenic Nanocomposites Prepared using a Novel Biphenyl-Containing Clay

Grace Chigwada
Marquette University

Dongyan Wang
Marquette University

David D. Jiang
Marquette University

Charles A. Wilkie
Marquette University, charles.wilkie@marquette.edu

Follow this and additional works at: https://epublications.marquette.edu/chem_fac

 Part of the Chemistry Commons

Recommended Citation

Chigwada, Grace; Wang, Dongyan; Jiang, David D.; and Wilkie, Charles A., "Styrenic Nanocomposites Prepared using a Novel Biphenyl-Containing Clay" (2006). *Chemistry Faculty Research and Publications*. 106.
https://epublications.marquette.edu/chem_fac/106

Marquette University

e-Publications@Marquette

Chemistry Faculty Research and Publications/College of Arts and Sciences

***This paper is NOT THE PUBLISHED VERSION;* but the author's final, peer-reviewed manuscript.** The published version may be accessed by following the link in th citation below.

Polymer Degradation and Stability, Vol. 91, No. 4 (April 2006): 755-762. DOI. This article is © Elsevier and permission has been granted for this version to appear in e-Publications@Marquette. Elsevier does not grant permission for this article to be further copied/distributed or hosted elsewhere without the express permission from Elsevier.

Styrenic Nanocomposites Prepared Using A Novel Biphenyl-Containing Modified Clay

Grace Chigwada
Department of Chemistry, Marquette University, Milwaukee, WI
Dongyan Wang
Department of Chemistry, Marquette University, Milwaukee, WI
David D. Jiang
Department of Chemistry, Marquette University, Milwaukee, WI
Charles A. Wilkie
Department of Chemistry, Marquette University, Milwaukee, WI

Abstract

Montmorillonite was organically modified using an ammonium salt containing 4-acetylbiphenyl. This clay (BPNC16 clay) was used to prepare polystyrene (PS), acrylonitrile butadiene styrene (ABS) and high impact polystyrene (HIPS) nanocomposites. Polystyrene nanocomposites were prepared both by in situ bulk polymerisation and melt blending processes, while the ABS and HIPS nanocomposites were prepared only by melt blending. X-ray diffraction and transmission electron microscopy were used to confirm nanocomposite formation. Thermogravimetric analysis was used to evaluate thermal stability and the flammability properties were evaluated using cone calorimetry. By thermogravimetry, BPNC16 clay was found to show high thermal stability, and by cone calorimetry, a decrease in both the peak heat release rate and the mass loss rate was observed for the nanocomposites.

Keywords

Polystyrene, Nanocomposites, Fire retardancy, Cone calorimetry, Surfactants

1. Introduction

Polymer nanocomposites are of great industrial as well as scientific interest and they have been used in various areas of transportation, construction and electrical products [1]. These applications are a result of the unusual combination of stiffness and strength offered by nanocomposites. The typical nano-material is clay, but graphite, single-wall and multiple-wall nanotubes and nanoscale spherical particles, such as polyhedral oligomeric silsesquioxane, POSS [2], [3], silica [4], [5], [6], and titania [7], [8], have also been used.

The focus of this work is on polymer–clay nanocomposites. Polymer layered silicate (PLS) nanocomposites are materials with dimensions typically in the range 1 nm–100 nm. These polymer nanocomposites attain a certain degree of stiffness, strength and barrier properties with far less inorganic content than that of comparable glass or mineral reinforced polymers [1]. Extensive work has been carried out in the polymer–clay nanocomposite field over the past two decades [9], [10], [11], [12], [13]. The compatibility, and thus the quality of the nano-dispersion, between the polymer and the clay has been a subject of much interest and has led to the development of new surfactants for the modification of the clay [14], [15], [16]. The commercial clay, Cloisite 10A (Southern Clay Products, Inc.), contains a single benzene ring and, in recent work from this laboratory, a clay containing a naphthyl substituent was described and this gives better dispersion in polystyrene than that is obtained with the commercial clay which contains a single benzene ring [17].

In this study, a larger substituent, 4-acetylbiphenyl was placed on the ammonium cation and this cation was used to modify the clay and polystyrene (PS), acrylonitrile butadiene styrene (ABS) and high impact polystyrene (HIPS) nanocomposites were prepared. The intention of this study is to determine how the different substituents affect the dispersion of the clay in the polymer.

2. Experimental

2.1. Materials

The majority of chemicals used in the study, including styrene, polystyrene, diethyl ether, tetrahydrofuran (THF), *N*,*N*-dimethylhexadecylamine, didecylmethylamine, and benzoyl peroxide (BPO), were obtained from the Aldrich Chemical Company, while α-bromo-4-phenylacetophenone (97%) was purchased from Alfa Aesar. Montmorillonite was kindly provided by Southern Clay Products, Inc. High impact polystyrene (HIPS) (Styron 438, melt flow index (MFI), 200 °C/5 kg, 4.5 g/10 min; Mw: 300 000) and acrylonitrile butadiene styrene (ABS) (Magnum 275, MFI, 230 °C/3.8 kg, 2.6 g/10 min; Mw: 160 000) were provided by Dow Chemical Company.

2.1.1. Preparation of phenylacetophenone dimethylhexadecyl ammonium (BPNC16) salt

The BPNC16 salt was prepared by the combination of α-bromo-4-phenylacetophenone and *N*,*N*-dimethylhexadecylamine. In a 250 ml flask was placed 7.0 g (25 mmol) α-bromo-4-phenylacetophenone in 100 ml THF. The mixture was stirred for a few minutes using a magnetic stirrer until a homogenous solution was formed. To this was gradually added 6.9 g (25 mmol) *N*,*N*-dimethylhexadecylamine and the mixture was stirred at RT. After a few hours, a white precipitate was formed. The solvent was removed and the sample was recrystallised from ether, leaving behind a white solid; the yield was 94%. ^{1}H NMR $CDCl_3$: δ 8.201 (d, J = 8.7, 2H), δ 7.639 (d, J = 8.4, 2H), δ 7.489–7.521 (m, 2H), δ 7.352–7.430 (m, 3H), δ 5.914 (s, 2H), δ 3.819–3.875 (m, 2H), δ 3.662 (s, 6H), δ 1.712–1.722 (m, 2H), δ 1.285–1.920 (m, 26H), δ 0.843 (t, J = 6.8, 3H).

2.1.2. Organic modification of the clay

A portion of the ammonium salt prepared by above method was dissolved in 100 ml of THF while the clay was dispersed in 200 ml of 2:1 water:THF; a 20% excess of the ammonium salt, based on the CEC of the clay, was used. These were mixed and stirred at room temperature for 24 h, followed by filtration and continuous washing with water until no chloride ion was detected using an aqueous silver nitrate solution.

2.1.3. Preparation of polymer–clay nanocomposites

Both bulk polymerisation and melt blending processes were utilized for the preparation of PS nanocomposites while ABS and HIPS nanocomposites were prepared only by melt blending. The procedures outlined in the literature [18] were used. Bulk polymerisation involves dispersing the clay in monomeric styrene, then adding initiator and carrying out the polymerisation by heating. Melt blending was performed using a Brabender mixer for 15 min at a temperature of about 190 °C at 60 rpm.

2.2. Instrumentation

X-ray diffraction (XRD) measurements were performed using a Rigaku powder diffractometer with a Cu tube source (λ = 1.54 Å); generator tension was 50 kV at a current of 20 mA. Scans were taken from 2ϑ = 1.0–10, step size = 0.1 and scan time per step of 10 s using the high-resolution mode. Bright field transmission electron microscopy (TEM) images of the composites were obtained at 60 kV with a Zeiss 10c electron microscope. The samples were ultramicrotomed with a diamond knife on a Reichert–Jung Ultra-Cut E microtome at room temperature to give ~70 nm thick section. The sections were transferred from the knife-edge to 600 hexagonal mesh Cu grids. Thermogravimetric analysis (TGA) was performed on a Cahn TG 131 unit under a flowing nitrogen atmosphere at a scan rate of 20 °C/min from 20 °C to 600 °C. All TGA experiments have been done in triplicate; the reproducibility of temperature is ±3 °C while amount of non-volatile residue is reproducible to ±2%. Cone calorimeter measurements at 35 kW m^{-2} were performed according to ASTM E 1354 using an Atlas Cone 2; the spark was continuous until the sample ignited. All samples were run in triplicate and the average value is reported. Results from cone calorimeter are generally considered to be reproducible to ±10% [19].

3. Results and discussion

The BPNC16 salt was prepared as outlined in Fig. 1 below and used for the organic modification of MMT. The objective of this study is to evaluate nanocomposite formation and flammability properties as a function of clay loading.

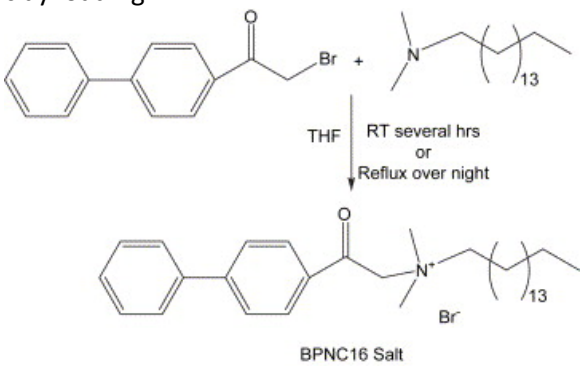

Fig. 1. Scheme for the preparation of BPNC16 salt.

3.1. XRD analysis

XRD of the modified clay showed 2ϑ of 3.7°, which corresponds to a d-spacing of 2.4 nm. This is a very large increase in the d-spacing compared to the original sodium MMT clay, which has a d-spacing of 1.2 nm. The clay was then used to prepare PS, HIPS and ABS nanocomposites. PS nanocomposites prepared by bulk polymerisation give a large increase in the d-spacing while those prepared by melt blending do not, as shown in Fig. 2. The d-spacing data, which is given in Table 1, shows that bulk polymerisation gives a d-spacing of

2.7 nm while there is no change in the d-spacing by melt blending, both the clay and the nanocomposite are at 2.4 nm. The lack of a change in the d-spacing may be attributed either to no nanocomposite formation or else the gallery space is already sufficiently large to permit the entry of polymer. Another technique is required to address this question.

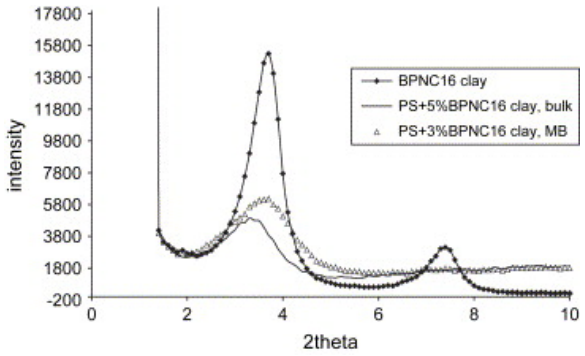

Fig. 2. XRD traces for polystyrene–BPNC16 nanocomposites; bulk means that the nanocomposite was prepared by bulk polymerisation while MB means that melt blending was used.

Table 1. XRD data for BPNC16 nanocomposites

Sample	**2ϑ**	**d-Spacing**
BPNC16 clay	3.7	2.4
PS + 3% BPNC16 clay, bulk	3.3	2.7
PS + 5% BPNC16 clay, bulk	3.3	2.7
PS + 3% BPNC16 clay, MB	3.7	2.4
PS + 5% BPNC16 clay, MB	3.7	2.4
ABS + 3% BPNC16 clay	2.9	3.0
HIPS + 3% BPNC16 clay	3.9	2.3

Fig. 3 shows the XRD traces for ABS and HIPS nanocomposites. A weak and diffuse peak is seen in ABS at slightly lower values of 2ϑ, larger d-spacing, while HIPS shows a weak and diffuse peak at slightly smaller d-spacing. For ABS an intercalated nanocomposite is indicated, while the breadth of the peak indicates that some disorder has likely occurred. For HIPS, disorder, and an immiscible system, is indicated by the XRD trace.

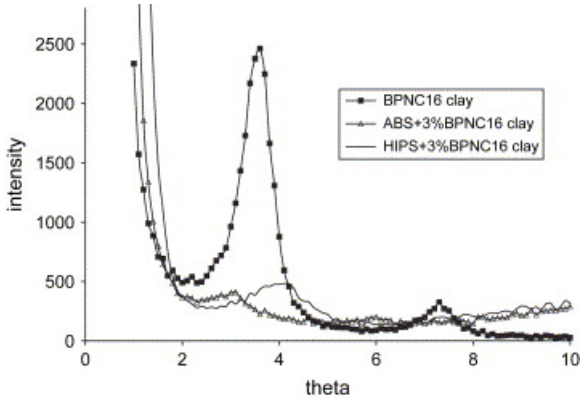

Fig. 3. XRD traces for ABS–BPNC16 and HIPS–BPNC16 nanocomposites prepared by melt blending.

3.2. Transmission electron microscopy (TEM)

In order to confirm the type of hybrid structure that has been formed, TEM images were obtained and these are shown in Fig. 4, Fig. 5 for the styrene nanocomposites. From the low magnification images it is evident that good dispersion was obtained in samples prepared both by bulk polymerisation and melt blending. This must indicate that the d-spacing of the clay alone was large enough to permit the entry of polymer without an

increase in the d-spacing. The high magnification images show small tactoids of a few to several clay layers and apparently suggest that intercalation has occurred.

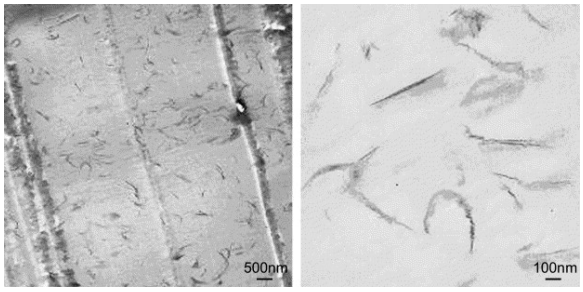

Fig. 4. TEM images for PS–BPNC16 nanocomposites prepared by bulk polymerisation; the low magnification image is on the left and the high magnification image on the right.

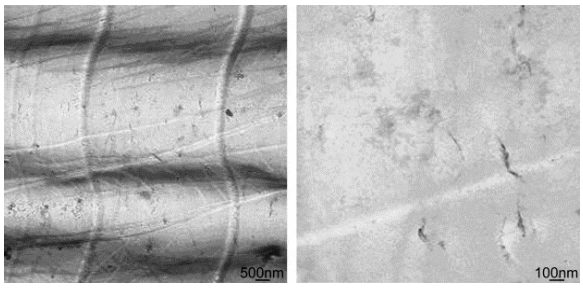

Fig. 5. TEM images for PS–BPNC16 nanocomposites prepared by melt blending; the low magnification image is on the left and the high magnification image on the right.

The TEM images for the ABS and HIPS nanocomposites are shown in Fig. 6, Fig. 7. The rubber phase is clearly evident in these images and one can see from the low magnification images that good dispersion has been obtained and both individual clay layers, as well as some small tactoids, can be seen. These may be described as mixed intercalated/delaminated nanocomposites.

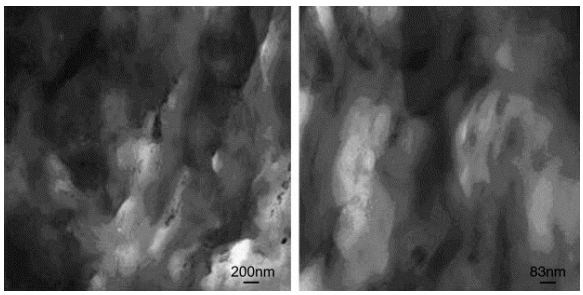

Fig. 6. TEM images for ABS–BPNC16 nanocomposites prepared by melt blending; the low magnification image is on the left and the high magnification image on the right.

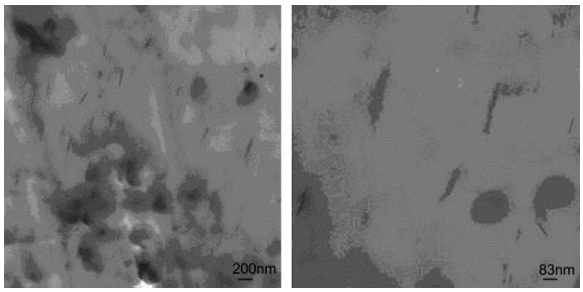

Fig. 7. TEM images for HIPS–BPNC16 nanocomposites prepared by melt blending; the low magnification image is on the left and the high magnification image on the right.

3.3. Thermogravimetric analysis

The thermal stability of both the clay and nanocomposites was examined by thermogravimetric analysis (TGA). The reported parameters include the temperature at which 10% degradation occurs, T_{10}, a measure of the onset of the degradation, the temperature at which 50% degradation occurs, T_{50}, the mid-point of the degradation, another measure of thermal stability, and the fraction of non-volatile residue at 600 °C, denoted as char; this data is given in Table 2 and the actual TGA curves are shown in Fig. 8, Fig. 9, Fig. 10, Fig. 11.

Table 2. Summary of TGA data for the styrenic-BPNC16 nanocomposites

Sample	T_{10}	T_{50}	**% Char**
BPNC16 clay	349 ± 2	–	71 ± 2
Commercial PS	400 ± 1	436 ± 0	0 ± 0
PS + 3% BPNC16 clay, bulk	425 ± 2	456 ± 2	5 ± 0
PS + 5% BPNC16 clay, bulk	427 ± 2	465 ± 2	4 ± 0
PS + 3% BPNC16 clay, MB	414 ± 1	452 ± 1	2 ± 0
PS + 5% BPNC16 clay, MB	417 ± 2	454 ± 2	5 ± 2
PS + 10% BPNC16 clay, MB	427 ± 2	460 ± 1	8 ± 3
Commercial ABS	423 ± 3	449 ± 1	1 ± 1
ABS + 3% BPNC16 clay	425 ± 3	454 ± 1	6 ± 1
ABS + 5% BPNC16 clay	424 ± 2	458 ± 2	7 ± 1
ABS + 10% BPNC16 clay	423 ± 1	460 ± 1	11 ± 3
Commercial HIPS	433 ± 1	459 ± 1	2 ± 2
HIPS + 3% BPNC16 clay, MB	439 ± 1	470 ± 1	10 ± 1
HIPS + 5% BPNC16 clay, MB	434 ± 0	466 ± 0	8 ± 1
HIPS + 10% BPNC16 clay, MB	437 ± 2	470 ± 1	12 ± 1

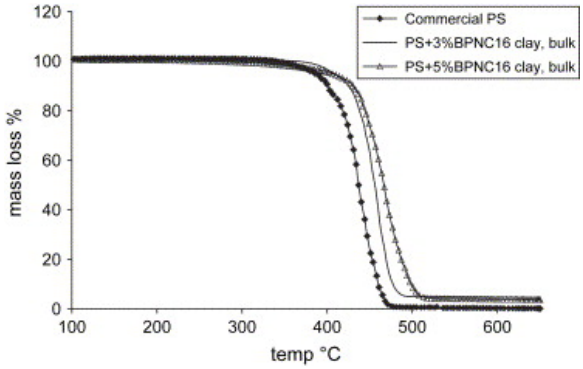

Fig. 8. TGA curves for PS–BPNC16 nanocomposites prepared by bulk polymerisation.

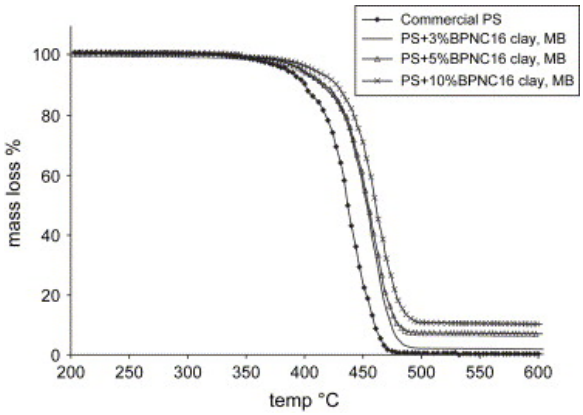

Fig. 9. TGA curves for PS–BPNC16 nanocomposites prepared by melt blending.

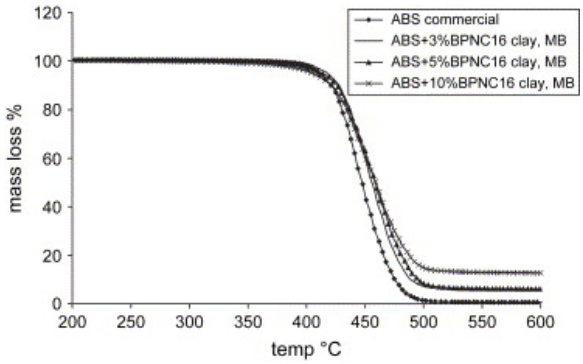

Fig. 10. TGA curves for ABS–BPNC16 nanocomposites prepared by melt blending.

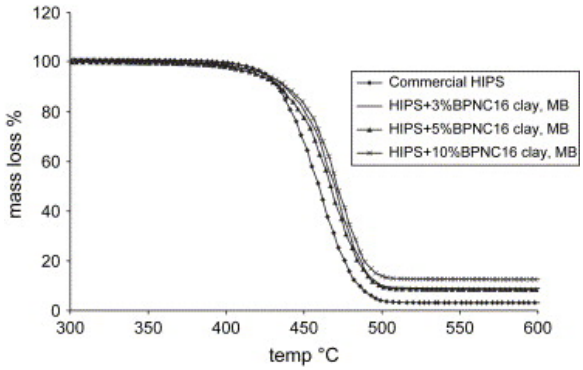

Fig. 11. TGA curves for HIPS–BPNC16 nanocomposites prepared by melt blending.

The organically modified clay exhibits high thermal stability compared to the commercial organically modified clays [16]; this clay has an onset temperature of degradation that is 20 °C–30 °C higher than that of the commercial materials. The nanocomposites prepared using this clay also showed significant improvements in both the onset and mid-point temperature of degradation. The amount of char was also significantly enhanced, which indicates that the presence of the clay can affect the degradation pathway and that the clay does play a role in the thermal degradation in an inert atmosphere.

Styrene nanocomposites were prepared both by melt blending and in situ polymerisation. Those prepared by melt blending process appear to have higher thermal stability than those prepared by in situ polymerisation; this is a surprising result since both appear to be well dispersed by TEM.

3.4. Cone calorimetry

An important observation that was made some time ago is that nanocomposite formation appears to offer an advantage in fire retardancy, particularly as studied by cone calorimetry. The parameters that may be evaluated from cone calorimetry include: the heat release rate, and especially its peak value, PHRR; the time to ignition, t_{ign}, and peak heat release rate, t_{PHRR}; specific extinction area (SEA), a measure of smoke; and the mass loss rate (MLR). One of the parameters that has been given special attention in fire retardancy is the peak heat release rate (PHRR), as this gives information about the size of the fire and thus the approximate fire hazard. In the literature, it has also been shown that nanocomposite gives rise to the maximum reduction in PHRR while a microcomposite formation gives essentially no reduction [19], [20]. This observation indicates that, apart from measuring fire properties, one can also obtain information about nano-dispersion from cone calorimetry. All of the cone data are summarized in Table 3. Some general observations can be made; the time to ignition uniformly decreases as does the peak heat release rate and the mass loss rate while the total heat released is unchanged and there is a small increase in the smoke produced. These are observations that are regularly seen in cone calorimetric studies of polymer–clay nanocomposites. The lack of a change in the total heat release is

significant because this indicates that the entire polymer does eventually burn but at a rate different from that of the virgin polymer.

Table 3. Summary of cone analysis for PS–BPNC16 nanocomposites

Sample	t_{ign}, s	PHRR, kW m^2 (% reduction)	t_{PHRR}, s	THR, MJ/m^2	ASEA, m^2/kg	MLR, g/sm^2
PS	65 ± 4	1298 ± 87	127 ± 21	100 ± 1	1186 ± 13	31 ± 1
PS + 3% BPNC16 clay, bulk	32 ± 5	784 ± 18 (40)	100 ± 6	82 ± 1	1295 ± 23	21 ± 1
PS + 5% BPNC16 clay, bulk	64 ± 5	646 ± 33 (50)	120 ± 4	83 ± 3	1308 ± 32	19 ± 1
PS + 3% BPNC16 clay, MB	60 ± 5	1015 ± 18 (22)	150 ± 7	91 ± 4	1279 ± 4	27 ± 1
PS + 5% BPNC16 clay, MB	60 ± 4	891 ± 49 (31)	153 ± 14	92 ± 2	1294 ± 6	26 ± 2
PS + 10% BPNC16 clay, MB	58 ± 2	772 ± 22 (41)	151 ± 151	88 ± 2	1314 ± 14	22 ± 1
ABS	71 ± 4	1036 ± 6	150 ± 6	100 ± 3	1155 ± 3	27 ± 1
ABS + 3% BPNC16 clay	60 ± 7	909 ± 15 (12)	143 ± 15	91 ± 6	1174 ± 17	25 ± 2
ABS + 5% BPNC16 clay	58 ± 3	853 ± 4 (18)	144 ± 4	91 ± 4	1225 ± 35	23 ± 1
ABS + 10% BPNC16 clay	60 ± 2	776 ± 15 (25)	144 ± 6	89 ± 3	1284 ± 31	21 ± 1
HIPS	71 ± 8	1082 ± 67	138 ± 25	96 ± 7	1225 ± 20	29 ± 2
HIPS + 3% BPNC16 clay	67 ± 2	973 ± 23 (10)	142 ± 9	94 ± 4	1283 ± 34	27 ± 1
HIPS + 5% BPNC16 clay	61 ± 3	970 ± 38 (10)	142 ± 6	95 ± 10	1276 ± 43	26 ± 1
HIPS + 10% BPNC16 clay	51 ± 5	844 ± 13 (22)	133 ± 5	92 ± 11	1321 ± 10	24 ± 1

t_{ign}, Time to ignition; PHRR, peak heat release rate; % reduction, [PHRR (polymer)−PHRR (nano)]/PHRR (polymer); t_{PHRR}, time to PHRR; THR, total heat released; ASEA, average specific extinction area; MLR, mass loss rate.

The heat release curves for polystyrene and its nanocomposites are shown in Fig. 12, Fig. 13. The samples prepared by bulk polymerisation show a larger reduction in the peak heat release rate than those prepared by melt blending. This contradicts the TEM observation that the nano-dispersion is as good for both samples and reinforces the need for some bulk measurement of nano-dispersion.

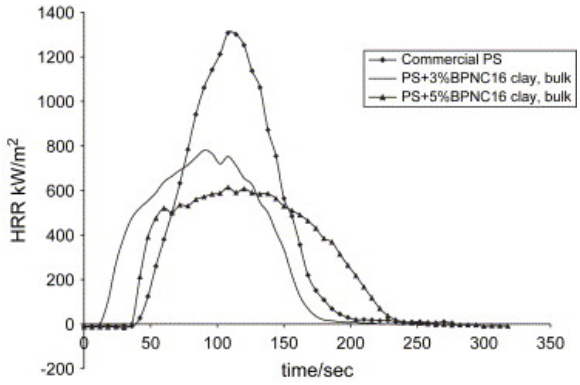

Fig. 12. Heat release rate curves for PS–BPNC16 nanocomposites prepared by bulk polymerisation.

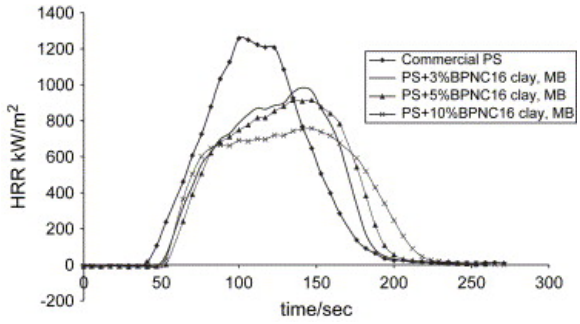

Fig. 13. Heat release rate curves for PS–BPNC16 nanocomposites prepared by melt blending.

The heat release rate curves for ABS and HIPS are shown in Fig. 14, Fig. 15. For both polymers, PHRR decreases as the amount of clay is increased, indicating the effectiveness of this clay in fire retardancy. For comparison, the best reduction in peak heat release rates that have been obtained for ABS and HIPS nanocomposites are 25% and 22%, respectively, and these are comparable to those values [16], [21], which indicate that good nano-dispersion has been achieved.

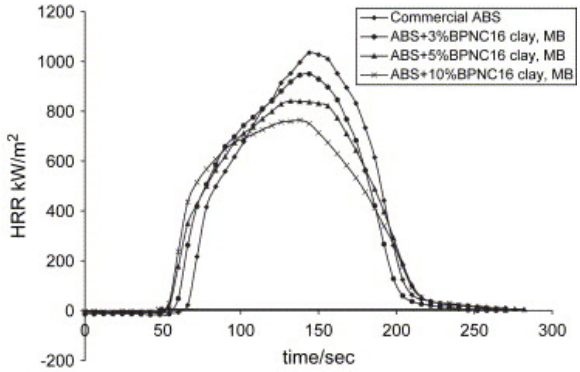

Fig. 14. Heat release rate curves for ABS–BPNC16 nanocomposites prepared by melt blending.

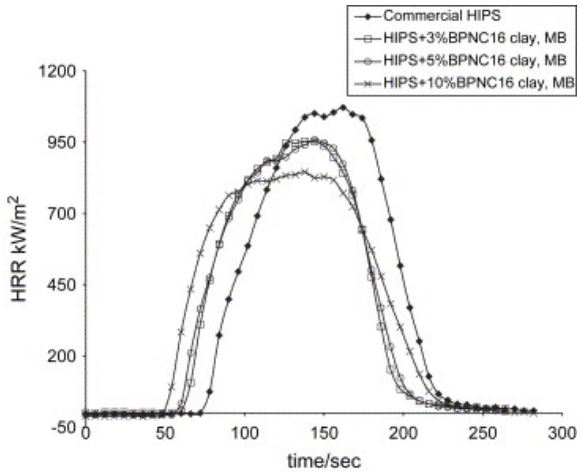

Fig. 15. Heat release rate curves for HIPS–BPNC16 nanocomposites prepared by melt blending.

4. Conclusions

BPNC16 modified clay has enhanced thermal stability and a larger d-spacing compared to some commercially available clays and it can be conveniently prepared in a few hours time at room temperature with a minimum amount of solvent, which makes it potentially economical and convenient. The nanocomposites prepared with this clay show improved thermal stability and a significant reduction in the peak heat release rate from cone calorimetric measurements.

References

[1] W. Xie, J.M. Hwu, G.J. Jiang, T.M. Buthelezi, W. Pan. *Polym Eng Sci*, 43 (2003), pp. 214-221

[2] Esker AR. Vastine BA, Deng J, Polidan JT, Viers BD, Satija SK. Abstracts of papers. 225th ACS national meeting, March 23–27, New Orleans, LA, United States; 2003.

[3] H. Xu, S.-W. Kuo, C.-F. Huang, F.-C. Chang. *J Polym Res*, 9 (2002), pp. 239-244

[4] M.J. Percy, V. Michailidou, S.P. Armes, C. Perruchot, J.F. Watts, S.J. Greaves. *Langmuir*, 19 (2003), pp. 2072-2079

[5] A.J. Waddon, Z.S. Petrovic. *Polym J (Tokyo, Japan),* 34 (2002), pp. 876-881

[6] Q. Zhang, L.A. Archer. *Langmuir*, 18 (2002), pp. 10435-10442

[7] S.X. Wang, L.D. Zhang, H. Su, Z.P. Zhang, G.H. Li, G.W. Meng, *et al. Phys Lett A*, 281 (2001), pp. 59-63

[8] N.R. de Tacconi, J. Carmona, W.L. Balsam, K. Rajeshwar. *Chem Mater*, 10 (1998), pp. 25-26

[9] Y. Kojima, A. Usuki, M. Kawasumi, A. Okada, Y. Fukushima, T. Kurauchi, *et al. J Mater Res*, 8 (1993), pp. 1185-1189

[10] V. Mehrotra, E.P. Giannelis. *Solid State Ionics*, 51 (1992), pp. 115-122

[11] T. Lan, P.D. Kaviratna, T.J. Pinnavaia. *Chem Mater*, 6 (1994), pp. 573-575

[12] J. Zhu, F.M. Uhl, A.B. Morgan, C.A. Wilkie. *Chem Mater*, 13 (2001), pp. 4649-4654

[13] S. Su, C.A. Wilkie. *J Polym Sci Polym Chem*, 41 (2003), pp. 1124-1135

[14] S. Su, D.D. Jiang, C.A. Wilkie. *Polym Degrad Stab*, 83 (2004), pp. 321-331

[15] J. Zhang, C.A. Wilkie. *Polym Degrad Stab*, 83 (2004), pp. 301-307

[16] X. Zheng, C.A. Wilkie. *Polym Degrad Stab*, 82 (2003), pp. 441-450

[17] Chigwada G, Jiang DD, Wilkie CA. In: Wilkie CA, Nelson GL, editors. *Fire and polymers. Materials and concepts for hazard prevention*; in press.

[18] D. Wang, J. Zhu, Q. Yao, C.A. Wilkie. *Chem Mater*, 14 (2002), pp. 3837-3843

[19] J.W. Gilman, T. Kashiwagi, M. Nyden, J.E.T. Brown, C.L. Jackson, S. Lomakin, S. Al-Maliaka, A. Golovoy, C.A. Wilkie (Eds.), *Chemistry and technology of polymer additives*, Blackwell Scientific, London (1998), pp. 249-265

[20] S. Su, D.D. Jiang, C.A. Wilkie. *J Vinyl Addit Technol*, 10 (2004), pp. 44-51

[21] S. Su, D.D. Jiang, C.A. Wilkie. *Polym Degrad Stab*, 84 (2004), pp. 279-288